

Characterization, NBO, NLO And Molecular Structural Analysis Of A Material -2-Hydroxyquinoline-4-Carboxylic Acid By Using DFT Method

Katta Eswar Srikanth¹, S Venkata Raju¹, M Satya Vani¹, D Vijay¹,
P Paul Divakar² & A Veeraiah^{1*}

¹Molecular Spectroscopy Laboratory, Department of Physics, D.N.R College (A),
Bhimavaram, A.P., India-534202

²Department of Physics, Sir C.R.R.College, Eluru, W.G.Dt., A.P-534006

Abstract : The most stable structure of 2-Hydroxyquinoline-4-carboxylic acid (2H4C) has been obtained at ground state. All the structural parameters of the titled compound are determined by DFT with B3LYP functional using 6-311++G** basis set. The fundamental vibrational modes are studied with use of theoretical vibrational spectra. The harmonic vibrational frequencies are theoretically calculated, presented and analysed. The frontier molecular orbitals such as highest occupied molecular orbital (HOMO) and lowest unoccupied molecular orbital (LUMO) energies are determined by using DFT/B3LYP/6-311++G** basis set. The electron density distribution and site of chemical reactivity of 2H4C molecule have been obtained by mapping electron density iso-surface with molecular electrostatic potential (MEP). Stability of the molecules arising from hyper conjugative interactions, charge delocalizations has been analyzed by using natural bond orbital (NBO) analysis. Hyperpolarizability calculations of the investigated compound show that the non-linear optical property of the 2H4C greater than the standard compound, Urea. The thermodynamic properties and atomic natural charges of the compound are analyzed and the reactive site of the molecule is identified. The global and local reactivity descriptors are evaluated.

Keywords: 2-Hydroxyquinoline-4-carboxylic acid, Density Functional Theory, NBO, MESP .

I. Introduction

Nitrogen based heterocyclic compounds play an important role in biomedical research and drug designing due to their immense potential against tumor cells [1]. Quinolone forms part of the structure of quinine found in cinchona bark and constitutes a wide variety of antibiotics, has antibacterial effect and is highly effective in the treatment of urinary tract infections [2]. Derivatives of isoquinolines are useful as bacteria-staining agents for microscopy, antiseptics such as the coal-tar dye acriflavine, antimalarial agents such as mepacrine(quinacrine) and chloroquine and antibacterial agents such as ciprofloxacin, trypanocides [3]. Some of the derivatives are found in natural products and found wide acceptance within the pharmaceutical industry due to its activity like anti-malarial [4], anti-hypertensive [5], antifungal [6], anti-microbial [7], anti-tumor [8], anti-diabetic, anti-oxidant and anti-hypertensive [9]. However, literature survey indicates that there are limited number of investigations on the vibrational spectra of Isoquinoline and its derivatives. In this study, we report theoretical vibrational, Raman and UV studies on 2-Hydroxyquinoline-4-carboxylic acid using DFT calculations for the first time.

II. Computational Details

The density functional calculations were carried out with GAUSSIAN 09W program packages [10]. The geometry of molecule was displayed using GaussView 5.0 program [11]. The molecular structure was optimized by using B3LYP [12-13] with the 6-311++G** basis set. Vibrational wavenumbers are obtained from the Gabedit software program. The NBO and NLO analysis were investigated by using DFT/B3LYP method with 6-311++G** basis set available in the NBO 3.1 in the Gauss view program.

III. Results And Discussion

3.1 Geometry optimization:

The optimized geometries in the ground state energy level were performed by B3LYP with the 6-311++G** basis set (Fig. 1). The optimized structural parameters of 2H4C were listed in [Table 1](#). In the bond lengths C7-C12 shows the highest theoretical value at 1.506 Å. All the remaining bond lengths are in good manner. In the case of bond angles C7-C12-O13 shows the higher bond angle value at 124.31 Å.

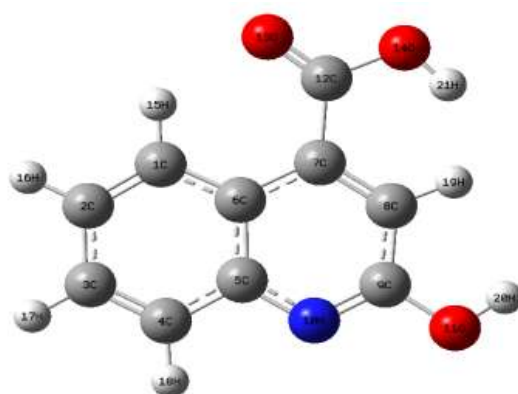


Fig.1: Optimized structure of 2-Hydroxyquinoline-4-carboxylic acid along with numbering scheme.

Table 1: Optimized geometrical parameters of 2-Hydroxyquinoline-4-carboxylic acid obtained by B3LYP/6-311++G** density functional calculations

Bond Length	Value(Å)	Bond Angle	Value(°)	Dihedral Angle	Value(°)
C1-C2	1.374	C1-C2-C3	120.55	C1-C2-C3-C4	0.130
C2-C3	1.413	C2-C3-C4	120.57	C2-C3-C4-C5	-0.055
C3-C4	1.374	C3-C4-C5	120.41	C3-C4-C5-C6	-0.156
C4-C5	1.416	C4-C5-C6	119.03	C4-C5-C6-C1	0.293
C5-C6	1.431	C5-C6-C1	119.17	C5-C6-C1-C2	-0.223
C6-C1	1.418	C6-C1-C2	120.25	C6-C1-C2-C3	0.012
C6-C7	1.427	C5-C6-C7	116.36	C5-C6-C7-C8	-1.002
C7-C8	1.376	C6-C7-C8	119.46	C6-C7-C8-C9	-0.671
C8-C9	1.422	C7-C8-C9	118.88	C7-C8-C9-N10	1.867
C9-N10	1.300	C8-C9-N10	123.67	C8-C9-N10-C5	-1.134
N10-C5	1.362	N10-C5-C6	123.01	C8-C9-O11-H29	2.753
C7-C12	1.506	O13-C12-O14	120.35	N10-C9-O11-H29	-177.57
C12-O13	1.198	C8-C9-O11	120.58	C8-C7-C12-O13	47.16
C12-O14	1.359	N10-C9-O11	115.75	C6-C7-C12-O14	-134.66
C9-O11	1.359	C5-C7-C12	121.37	C6-C7-C12-O13	46.57
O14-H21	0.965	C8-C7-C12	119.14	C6-C7-C12-O14	-134.66
C1-H15	1.081	C6-C1-H15	119.43	O13-C12-C14-H21	-172.54
C2-H16	1.083	C2-C1-H15	120.34		
C3-H17	1.082	C1-C2-H16	119.75		
C4-H18	1.082	C3-C2-H16	119.69		
C8-H19	1.085	C2-C3-H17	119.54		
O11-H20	0.963	C4-C3-H17	119.88		
		C3-C4-H18	121.93		
		C5-C4-H18	117.65		
		C7-C8-H19	120.93		
		C9-C8-H19	120.12		
		C9-O11-H20	110.28		
		C7-C12-O13	124.31		
		C7-C12-O14	115.32		
		C12-C14-H21	110.26		

3.2 Natural bonding orbital analysis:

The NBO analysis provides an efficient method for understanding of intra- and inter-molecular bonding, bond species and interactions among bonds. Additionally, it is used for investigating of hyperconjugation interactions (charge transfers (ICT)) between Lewis type (bonding or lone pair) filled orbitals and non-Lewis type (antibonding and Rydberg) vacancy orbitals in molecular systems. The $E^{(2)}$ that is the energy of hyperconjugative interactions (stabilization energy) shows the interaction between donor groups and acceptor ones. Delocalization of electron density between occupied Lewis type orbitals and formally unoccupied non-Lewis orbitals corresponding to a stabilizing donor-acceptor interaction. For each donor NBO (i) and acceptor NBO (j), the stabilization energy $E^{(2)}$ associated with electron delocalization between donor and acceptor is estimated as [14]

$$E^{(2)} = -n_{\sigma} \frac{\langle \sigma | F | \sigma \rangle^2}{\epsilon_{\sigma^*} - \epsilon_{\sigma}} = -n_{\sigma} \frac{F_{ij}^2}{\Delta E} \quad (1)$$

Where, or F_{ij}^2 is the Fock matrix element i and j NBO orbitals, ϵ_{σ^*} and ϵ_{σ} are the energies of σ and σ^* NBOs and n_{σ} is the population of the donor σ orbital. The larger is the $E^{(2)}$ value, the more intensive is the interaction between electron donors and electron acceptors, i.e. the more donating tendency from electron donors to electron acceptors and the greater the extent of conjugation of the whole system. The results of second-order perturbation theory analysis of the Fock Matrix at B3LYP/6-311++G** level of theory are presented in [Table 2](#).

Table 2: Second order perturbation theory analysis of Fock Matrix in NBO basis for 2-Hydroxyquinoline-4-carboxylic acid

Donor(i)	Type	Ed/e	Acceptor(j)	Type	Ed/e	E ⁽²⁾	E(i)-E(j)	F (i, j)
C1-C2	σ	1.97875	C3-H17	σ^*	1.98117	2.78	1.14	0.050
	σ		C6-C7	σ^*	1.97017	3.59	1.20	0.059
C1-C6	σ	1.97327	C5-C6	σ^*	1.96822	3.42	1.19	0.057
			C5-N10	σ^*	1.97661	3.82	1.21	0.061
			C6-C7	σ^*	1.97017	3.99	1.19	0.062
C1-C6	π	1.55435	C2-C3	π^*	1.98049	18.95	0.28	0.066
			C4-C5	π^*	1.96788	21.64	0.28	0.070
			C7-C8	π^*	1.72978	24.36	0.24	0.070
C1-H15	σ	1.97903	C2-C3	σ^*	1.57150	4.07	1.10	0.060
C2-C3	σ	1.98049	C3-C4	σ^*	1.97745	2.58	1.28	0.051
C2-C3	π	1.57150	C1-C6	π^*	1.55435	22.97	0.27	0.071
			C4-C5	π^*	1.52420	19.23	0.29	0.066
C2-H16	σ	1.97976	C1-C6	σ^*	1.97327	4.27	1.05	0.060
			C3-C4	σ^*	1.97745	3.54	1.08	0.055
C3-C4	σ	1.97745	C4-C5	σ^*	1.96788	3.11	1.25	0.056
			C5-N10	σ^*	1.97661	3.05	1.21	0.054
C3-H17	σ	1.98117	C1-C2	σ^*	1.97875	3.57	1.10	0.056
C4-C5	σ	1.96788	C5-C6	σ^*	1.96822	4.37	1.21	0.065
C4-C5	π	1.52420	C1-C6	π^*	1.55435	18.01	0.27	0.063
	π		C2-C3	π^*	1.57150	21.66	0.28	0.067
	π		C9-N10	π^*	1.73374	22.19	0.24	0.038
C4-H18	σ	1.97786	C5-C6	σ^*	1.96822	4.73	1.01	0.062
C5-C6	σ	1.96822	C4-C5	σ^*	1.96788	5.15	1.25	0.072
C5-N10	σ	1.97661	C9-O11	σ^*	1.98176	3.41	1.17	0.057
C6-C7	σ	1.97017	C7-C8	σ^*	1.97194	3.47	1.23	0.058
C7-C8	σ	1.72978	C1-C6	π^*	1.55435	14.56	0.31	0.063
	σ		C9-N10	π^*	1.73374	27.18	0.28	0.080
C8-C9	σ	1.98213	C7-C8	σ^*	1.97194	3.39	1.29	0.059
C8-H19	σ	1.97630	C9-N10	σ^*	1.98176	4.79	1.10	0.065
C9-N10	σ	1.98176	C8-C9	σ^*	1.98213	3.18	1.39	0.060
C9-N10	π	1.73374	C4-C5	π^*	1.52420	23.49	0.35	0.084
			C7-C8	π^*	1.72978	13.35	0.31	0.058
C12-O13	π	1.97740	C7-C8	π^*	1.72978	5.13	0.38	0.043
C12-O14	σ	1.99578	C12-O13	π^*	1.97740	88.97	2.85	0.478
			C12-O14	σ^*	1.99578	138.15	3.36	0.622
C12-O13	π	1.97740	C12-O14	σ^*	1.99578	26.92	0.51	0.259
O14	LP	1.97230	C12-O14	σ^*	1.99578	183.45	20.87	1.857

The strong intramolecular hyperconjugation interactions or intramolecular charge transfers (ICT) are found in σ to σ^* , π to π^* , n to σ^* and n to π^* transitions. The strongest hyperconjugation interaction is from the lone pair n electrons of O14 atoms to antibonding σ^* electrons of C12-O14 bond. Similarly the interaction between σ of C12-O14 and O14(LP) to σ^* of C12-O14 has the most stabilization energy 138.15, 183.45 kcalmol⁻¹ respectively. The interaction between the σ of C2-C3 to the σ^* of C3-C4 which has the stabilization energy 2.58 kcalmol⁻¹ represents the least stabilization energy within the molecule.

3.3. Polarizability and first order hyperpolarizability:

Non-linear optical (NLO) materials find applications in wide area like telecommunications, signal processing

and optical inter-connections, in providing key functions of frequency shifting, optical switching, optical logic and optical memory [15-17]. NLO material gives rise to new fields when interacts with the incident electromagnetic field that undergoes a change in phase, frequency, amplitude or other propagation characteristics [18]. NLO behaviour of a material can be studied by measuring the total dipole moment and first order hyperpolarizability. The non-linear optical response of an isolated molecule in an electric field can be expressed as a Taylor series expansion of the total dipole moment, μ_t , induced by the field:

$$\mu_t = \mu_0 + \alpha_{ij}E_j + \beta_{ijk}E_jE_k + \dots \quad (2)$$

where, μ_0 is the permanent dipole moment, α_{ij} are the components of polarizability, β_{ijk} are the components of the first order hyperpolarizability.

The first order hyperpolarizability is a third rank tensor. Hence, it contains 27 components represented by a 3 x 3 x 3 matrix. Due to Klienman symmetry [19], the 27 components get reduced to 10 components ($\beta_{xyx} = \beta_{yyx} = \beta_{yyx} = \beta_{zyz} = \beta_{zyz}, \dots$). Similarly other permutation of x, y, z subscripts also take same value). These components are:

$$\beta_{xxx}, \beta_{xxy}, \beta_{xyx}, \beta_{yyy}, \beta_{xzz}, \beta_{xyz}, \beta_{yyz}, \beta_{xzz}, \beta_{yzz}, \beta_{zzz}$$

They can be calculated using the following equation [20]:

$$\beta_i = \beta_{iii} + (1/3) \sum_{i \neq j} (\beta_{ijj} + \beta_{jij} + \beta_{jji}) \quad (3)$$

The total static dipole moment (μ_t), the isotropic (or average) linear polarizability (α_t), the anisotropy of polarizability ($\Delta\alpha$), and the mean first order hyperpolarizability (β_t), using the x, y, z components are defined as:

$$\mu_t = (\mu_x^2 + \mu_y^2 + \mu_z^2)^{1/2} \quad (4)$$

$$\alpha_t = (\alpha_{xx} + \alpha_{yy} + \alpha_{zz})/3 \quad (5)$$

$$\Delta\alpha = 2^{-1/2} [(\alpha_{xx} - \alpha_{yy})^2 + (\alpha_{yy} - \alpha_{zz})^2 + (\alpha_{zz} - \alpha_{xx})^2 + 6\alpha_{xx}^2]^{1/2} \quad (6)$$

$$\beta_t = (\beta_x^2 + \beta_y^2 + \beta_z^2)^{1/2} \quad (7)$$

where,

$$\beta_x = \beta_{xxx} + \beta_{xyy} + \beta_{xzz}$$

$$\beta_y = \beta_{yyy} + \beta_{xxy} + \beta_{yzz}$$

$$\beta_z = \beta_{zzz} + \beta_{xxz} + \beta_{yyz}$$

The value of hyperpolarizability of a molecule is a measure of NLO activity. It is associated with intramolecular charge transfer that arises from the electron cloud movement through π -conjugated framework of electrons [21]. Consequently, DFT has been employed to study the NLO behavior of some materials [22-23] in our earlier work. DFT/B3LYP/6-311++G** level of theory has been used to compute the total molecular dipole moment (μ_t) and its components; total molecular polarizability (α_t) and its components; first order hyperpolarizability (β_t) and its components. The results are reported in Table 3. The NLO behaviour of a molecule is normally determined by comparing its total molecular dipole moment (μ_t) and mean first order hyperpolarizability with corresponding values of Urea for which μ_t is 1.3732 Debye and β_t is $0.3728 \times 10^{-30} \text{ cm}^5/\text{esu}$. For the molecule 2H4C, the value of μ_t is 0.9349 Debye and β_t is $3.92578 \times 10^{-30} \text{ cm}^5/\text{esu}$. From the above values, it can be seen that the values of μ_t and β_t of 2H4C are greater than that of Urea. Hence, it demonstrates that 2H4C exhibits NLO properties.

Table 3: The electric dipole moment (D), average polarizability, first hyperpolarizability, etc., of 2-hydroxyquinoline-4-carboxylic acid 1 polar by B3LYP/6-311++G**

μ and α components	B3LYP/6-311++G**	β components	B3LYP/6-311++G**
μ_x	0.9447009	β_{xxx}	-77.6450021
μ_y	-0.2059772	β_{xxy}	213.484495
μ_z	-0.0072926	β_{xyy}	113.0155344
$\mu_{(D)}$	0.9349395	β_{yyy}	255.4332896
α_{xx}	196.8758142	β_{xzz}	-0.2912306
α_{xy}	7.8728923	β_{xyz}	0.220515
α_{yy}	152.8270474	β_{yyz}	0.0086594
α_{xz}	-0.0126329	β_{xzz}	-55.1313003
α_{yz}	0.0466699	β_{yzz}	-14.9380978
α_{zz}	67.503236	β_{zzz}	-0.475063

$\Delta\alpha$	50.96362 x 10 ⁻²⁴ esu		
(esu)	20.70161 x 10 ⁻²⁴ esu	β total (esu)	3.92578 x 10 ⁻³⁰ esu

3.4 Frontier molecular orbitals:

The Highest Occupied Molecular Orbital's (HOMOs) and Lowest Unoccupied Molecular Orbitals (LUMOs) are named Frontier molecular orbital's (FMOs). The atomic orbital compositions of the frontier molecular orbital are shown in Fig.2. Gauss-Sum 2.1 Program [24] was used to calculate the group contributions to the molecular orbital's (HOMO and LUMO) and prepare the density of the state (DOS) as shown in Fig.3. The DOS spectra were created by convoluting the molecular orbital information with the Gaussian curves of unit height. The HOMO-LUMO energy gap of 2H4C was calculated at B3LYP level with 6-311++G** basis set and is presented in Table 4. The LUMO as an electron acceptor represent the ability to obtain an electron, HOMO represents the ability to donate an electron [25]. The energy gap of HOMO-LUMO explains the eventual charge transfer interaction within the molecule, which influences the biological activity of the molecule. The positive and negative phase is represented in red and green color, respectively. The energy values of HOMO and LUMO are 5.8202 eV and 1.2003 eV respectively and the HOMO-LUMO energy gap values is 6.82434 eV for B3LYP level with 6-311++G** basis set. The most widely used theory by chemists is the molecular orbital (FMOs) theory. It is important that Ionization potential (I), Electron affinity (A), Electrophilicity (ω), Chemical potential (μ), Electronegativity (χ), Hardness (η), and Softness (σ) be put into a MO framework. We focus on the HOMO and LUMO energies in order to determine the interesting molecular (atomic) properties and chemical quantities. In simple molecular orbital theory approaches, the HOMO energy is related to the ionization potential (I) and the LUMO energy has been used to estimate the electron affinity (A) respectively by the following relations:

(8)

$$\mu = \frac{-(I + A)}{2} \quad (9)$$

$$\chi = \frac{I + A}{2} \quad (10)$$

The softness is the inverse of the hardness $S = \frac{1}{\eta}$. Parr et al.[58] introduced the global electrophilicity (ω) in

terms of chemical potential and hardness as $\omega = \frac{\mu^2}{2\eta}$

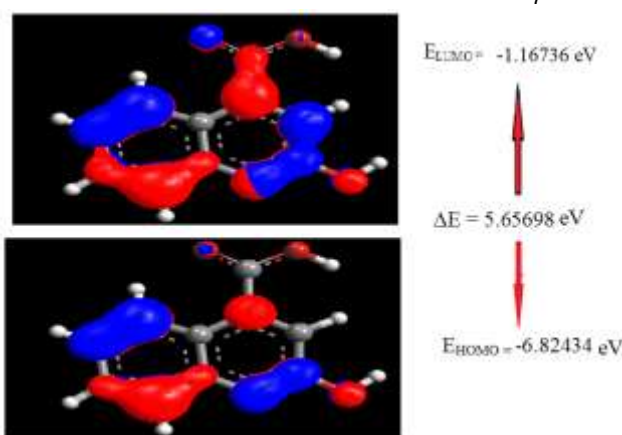


Fig. 2: The atomic orbital components of the frontier molecular orbital
2H4C
(HOMO—MO: 49, LUMO—MO: 50) of 2H4C

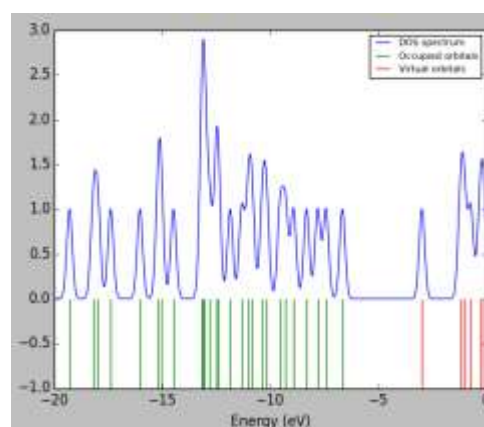


Fig.3: DOS spectra of

Table 4: The calculated quantum chemical parameters for 2-Hydroxyquinoline-4-carboxylic acid obtained by B3LYP/6-311++G** calculations.

Property	2-Hydroxyquinoline-4-carboxylic acid
Total energy (eV)	-18120.19
E_{HOMO} (eV)	-6.82434
E_{LUMO} (eV)	-1.16736

$E_{\text{HOMO}}-E_{\text{LUMO}}$ (eV)	5.65698
Ionization potential(I) (eV)	6.82434
Electron Affinity(A) (eV)	1.16736
Chemical potential (μ) (eV)	-3.99585
Electronegativity (χ)eV	3.99585
Chemical hardness(η)eV	-2.82849
Electrofilicity index (ω) eV	-2.82245
Global Softness (σ)eV	-0.35425
Total energy change(ΔE_T) eV	-0.70712
Dipole moment(D)	2.2475

3.5 Theoretical UV-Visible spectrum:

Theoretical UV-Visible spectra of the investigated compound was calculated by using TD-DFT/B3LYP/6-311++G** level of theory. The absorption maximum was observed at 323 nm, 425 nm respectively which was shown in Fig. 4. The percentage of major contribution of HOMO and LUMO along with oscillator strength and energy were tabulated in Table 5

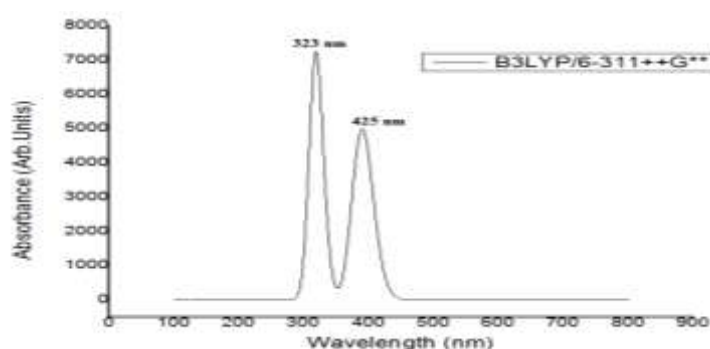


Fig.4. Theoretical UV/Vis spectra of 2-Hydroxyquinoline-4-carboxylic acid

Table 5: The UV-Vis excitation energy and oscillator strength for 2-Hydroxyquinoline-4-carboxylic acid calculated by TD-DFT/B3LYP/6-311++G** method.

S.No.	Energy (cm ⁻¹)	Wavelength (nm)	Osc. Strength	Symmetry	Major contribs
1	30301.65	425.09	0	Singlet-A	H-2->LUMO (89%)
2	33673.07	323.30	0.0735	Singlet-A	H-1->LUMO(48%),HOMO->LUMO(-40%)
3	35059.55	315.01	0.4212	Singlet-A	H-1->LUMO(40%),HOMO->LUMO (39%)
4	37532.46	296.97	0	Singlet-A	H-3->LUMO (96%)
5	38238.2	285.22	0.023	Singlet-A	H-4->LUMO (94%)

3.6 MESP analysis:

The molecular electrostatic potential (MESP) is widely used as a reactivity map displaying most probable regions for the electrophilic attack of charged point-like reagents on organic molecules [26, 27]. The molecular electrostatic potential (MESP) $V(r)$ at a point r due to a molecular system with nuclear charges $\{ZA\}$ located at $\{RA\}$ and the electron density $\rho(r)$ is given by

$$V(r) = \sum N A \left[\frac{ZA}{|r-RA|} \right] - \int \rho(r') d3r' / |r-r'| \quad (10)$$

Where, N denotes the total number of nuclei in the molecule and the two terms refer to the bare nuclear potential and the electronic contributions, respectively. The balance of these two terms brings about the effective localization of electron-rich regions in the molecular system. The MESP topography is mapped by examining the eigen value of the Hessian matrix at the point where the gradient $V(r)$ vanishes.

Molecular electrostatic potential maps of the compound was computed using B3LYP functional with 6-311++G** basis set. The 3D dimensional representation of the molecule was represented in Fig.5. From the figure we have observed that the red color region was the nucleophilic region so that was involved in electrophilic substitution in the chemical reaction and blue color indicates the electrophilic region therefore that region was involved in nucleophilic substitution in the chemical reaction. No electrostatic potential at the region was indicated by pink color.

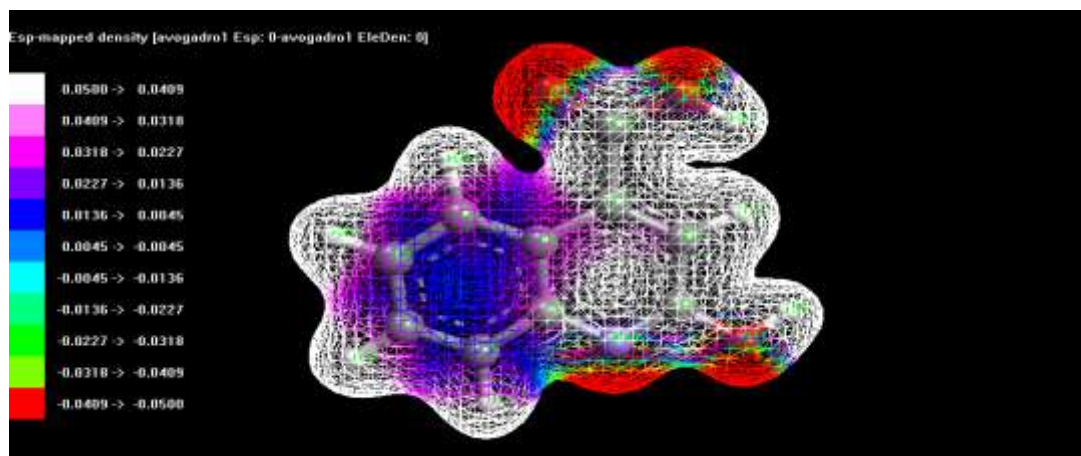


Fig. 5: B3LYP/6-311++G** calculated 3D molecular electrostatic potential maps 2H4C

3.7 Mulliken atomic charge population analysis:

Charge distributions of the molecules have been calculated by performing Mulliken analysis [28]. The theoretically calculation of atomic charges plays an important role in the application of quantum mechanical calculations to molecular systems. The calculated results are tabulated in Table 6 and from table it reveals that the negative charge is delocalized between carbon, oxygen and nitrogen atoms. In 2H4C molecule, the atoms constituting the hydrogen bonds possess the positive charges [29]. While some of the carbon atoms in the molecule have negative charges which form the hydrogen bonds, very similar values of positive charges are noticed for the four hydrogen pairs. The graphical representation of mulliken atomic charges was represented in Fig.6.

Table 6: Atomic charges for optimized geometry 2-Hydroxyquinoline-4-carboxylic acid at B3LYP/6-311++G** level

S.No.	Atom	Mulliken
1	C	-0.35411
2	C	-0.45647
3	C	-0.23304
4	C	-0.57108
5	C	-0.9329
6	C	0.854723
7	C	1.616029
8	C	-0.57078
9	C	-0.03713
10	N	-0.04256
11	O	-0.15564
12	C	-0.1852
13	O	-0.20346
14	O	-0.10921
15	H	0.157532
16	H	0.170466
17	H	0.174429
18	H	0.198459
19	H	0.184492
20	H	0.26836
21	H	0.227092

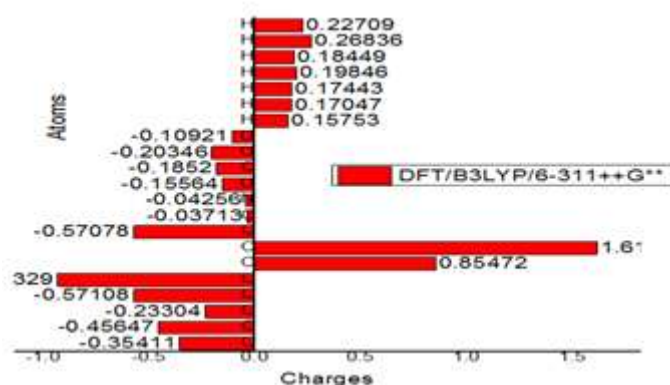


Fig 6: Graphical representation of mulliken charges of 2H4C

3.8 Thermodynamic properties:

The values of some thermodynamic parameters (such as zero point vibrational energy, thermal energy, specific heat capacity, rotational constants and entropy) of 2H4C at 298.15 K in ground state were calculated by B3LYP methods with 6-311++G** basis set and was listed in Table 7. The variation in Zero-Point Vibrational Energies (ZPVEs) seems to be significant. The calculated value of ZPVE of 2H4C was 109.5674 kcal/mol obtained by B3LYP with 6-311++G** basis set respectively.

Table 7: Thermodynamic parameters (for one mole of perfect gas at oneatm) and rotational constants of 2H4C

Thermodynamic parameter	2H4C
SCF Energy (Hartree)	-665.90473
Total energy (thermal), E_{total} (Kcal mol ⁻¹)	118.2932
Heat capacity at const. volume, c_v (cal mol ⁻¹ k ⁻¹)	40.306
Entropy, S (cal mol ⁻¹ k ⁻¹)	95.962
Vibrational energy, E_{vib} (kcal mol ⁻¹)	102.699
Zero-point vibrational energy, E_0 (kcal mol ⁻¹)	109.5674
Rotational constants	
A (GHz)	0.8342
B (GHz)	0.4053
C (GHz)	0.2968

IV. Conclusions

Geometry optimization has yielded structure parameters and the molecule 2H4C assumed C1 point group symmetry. The NBO analysis was made to understand the molecular structure by studying the interaction between the localized bonding and anti-bonding orbitals; electron delocalization and intra-molecular charge transfer (ICT). The study of dipole moment and hyper polarizability demonstrates that the molecule 2H4C exhibits NLO property, and hence it may be a potential applicant in the development of NLO materials. The high band gap between the frontier molecular orbitals demonstrates that the molecule 2H4C has high biological activity. Further, the title compound 2H4C is a good material for energy and doesn't harm environment.

Acknowledgements

The corresponding author, A.Veeraiah is highly grateful to Science and Engineering Research Board, Department of Science and Technology, Government of India (Project code- SB/EMEQ/2014) and Management of D.N.R.College Association for their financial and administrative support respectively.

References

- [1]. P. Martins, J. Jesus, S. Santos, L.R. Raposo, C. Roma-Rodrigues Pedro Viana Baptista and A.R. Fernandes, Heterocyclic Anticancer Compounds: Recent Advances and the Paradigm Shift towards the Use of Nanomedicine's Tool Box, *Molecules*, 20(9), 2015, 16852-16891
- [2]. R. Ridley, Medical need, scientific opportunity and the drive for antimalarial drugs, *Nature*, 415, 2002, 686-693.
- [3]. <https://www.britannica.com/science/heterocyclic-compound/Six-membered-rings-withone-heteroatom>
- [4]. W.A. Creasey, Biochemical effects of berberine, *Biochemical Pharmacology*, 28,1979, 1081-1084.
- [5]. J. Liu, P. Chan, Y. Chen, B. Tomlinson, S. Hong, The antihypertensive effect of the berberine derivative 6-protoberberine in

- spontaneously hypertensive rats, *Pharmacology*, 59(6), 1999, 283-289.
- [6]. T.C. Birdsall, Berberine: Therapeutic potential of an alkaloid found in several medicinal plants, *Alternative Medicine Review*, 2, 1997, 94-103.
- [7]. J. Zhou, S. Zhou, J. Tang, K. Zhang, L. Guang, Y. Huang, Y. Xu, Y. Ying, L. Zhang, D.Li, Protective effect of berberine on beta cells in streptozotocin- and highcarbohydrate/high-fat diet-induced diabetic rats, *European Journal of Pharmacology*, 606, 2009, 262-268.
- [8]. K. Zee-Cheng, K. Paull, Experimental antileukemic agents. Coralyne, analogs, and related compounds, *Journal of Medicinal Chemistry*, 17, 1974, 347-351.
- [9]. R. Gupta, W. Murray, R. Gupta, Cross resistance pattern towards anticancer drugs of a human carcinoma multidrug-resistant cell line, *British Journal of Cancer* 58, 1988, 441-447.
- [10]. M. J. Frisch, G. W. Trucks, H. B. Schlegel, G. E. Scuseria, M. A. Robb, J. R. Cheeseman, G. Scalmani, V. Barone, B. Mennucci, G. A. Petersson, H. Nakatsuji, M. Caricato, X. Li, H. P. Hratchian, A. F. Izmaylov, J. Bloino, G. Zheng, J. L. Sonnenberg, M. Hada, M. Ehara, K. Toyota, R. Fukuda, J. Hasegawa, M. Ishida, T. Nakajima, Y. Honda, O. Kitao, H. Nakai, T. Vreven, J. A. Montgomery, Jr., J. E. Peralta, F. Ogliaro, M. Bearpark, J. J. Heyd, E. Brothers, K. N. Kudin, V. N. Staroverov, R. Kobayashi, J. Normand, K. Raghavachari, A. Rendell, J. C. Burant, S. S. Iyengar, J. Tomasi, M. Cossi, N. Rega, J. M. Millam, M. Klene, J. E. Knox, J. B. Cross, V. Bakken, C. Adamo, J. Jaramillo, R. Gomperts, R. E. Stratmann, O. Yazyev, A. J. Austin, R. Cammi, C. Pomelli, J. W. Ochterski, R. L. Martin, K. Morokuma, V. G. Zakrzewski, G. A. Voth, P. Salvador, J. J. Dannenberg, S. Dapprich, A. D. Daniels, Ö. Farkas, J. B. Foresman, J. V. Ortiz, J. Cioslowski, and D. J. Fox, Gaussian 09W, Revision D.01, Gaussian, Inc., Wallingford CT, 2009.
- [11]. A. Frisch, A. B. Nielsen, A. J. Holder, Gaussview User's Manual Gaussian Inc., Pittsburg.
- [12]. A. D. Becke, Density-functional exchange-energy approximation with correct asymptotic-behavior, *Physical Review A*, 38, 1988, 3098-100
- [13]. C. Lee, W. Yang, R.G. Parr, Development of the Colle-Salvetti correlation-energy formula into a functional of the electron density, *physical review B*, 37, 1988, 785.
- [14]. Wienhold F, Landis CR, Valency and Bonding-A Natural Bond Orbital Donor-Acceptor Perspective, Cambridge University Press, New York, 2005.
- [15]. V. M. Geskin, C. Lambert, J. L. Bredas, Origin of high second-and third-order nonlinear optical response in ammonio/borato diphenylpolyene zwitterions: the remarkable role of polarized aromatic groups, *Journal of the American Chemical Society*, 125, 2004, 15651-15658.
- [16]. M. Nakano, H. Fujita, M. Takahata, K. Yamaguchi, Theoretical Study on Second Hyperpolarizabilities of Phenylacetylene Dendrimer: Toward an Understanding of Structure-Property Relation in NLO Responses of Fractal Antenna Dendrimers, *Journal of the American Chemical Society*, 124, 2002, 9648-9655
- [17]. D. Sajan, H. Joe, V. S. Jayakumar, J. Zaleski, Structural and electronic contributions to hyperpolarizability in methyl p-hydroxy benzoate, *Journal of molecular structure*, 785, 2006, 43-53.
- [18]. Y. X. Sun, Q. L. Hao, W. X. Wei, Z. X. Yu, L. D. Lu, X. Wang, Y. S. Wang, Experimental and Density Functional Studies on 4-(3,4-Dihydroxybenzylideneamino)antipyrine, and 4-(2,3,4-Trihydroxybenzylidene-amino)Antipyrine, *Journal of Molecular Structure THEOCHEM*, 904, 2009, 74-82.
- [19]. D. A. Klienman, Nonlinear Dielectric Polarization in Optical Media, *Physical Review*, 126, 1962, 1977.
- [20]. R. Zhang, B. Du, G. Sun, Y. X. Sun, Experimental and Theoretical Studies on o-, m- and p-Chlorobenzylideneaminoantipyrines, *Spectrochimica Acta part A: Molecular and Biomolecular Spectroscopy*, 75, 2002, 1115-1124.
- [21]. N. Prabavathi, N. Senthil Nayaki, B. Venkatram Reddy, Spectroscopic Investigation (FT-IR, FT-Raman, NMR and UV-Vis), Conformational Stability, NBO and Thermodynamic Analysis of 1-(2-Methoxyphenyl) Piperazine and 1-(2-Chlorophenyl) Piperazine by DFT Approach, *Spectrochimica Acta part A: Molecular and Biomolecular Spectroscopy*, 136, 2015, 1134-1148.
- [22]. J. Laxman Naik, B. Venkatram Reddy, N. Prabavathi, Experimental (FTIR and FT-Raman) and theoretical investigation of some pyridine-dicarboxylic acids, *Journal of molecular structure*, 1100, 2015, 43-58.
- [23]. N. Choudhary, S. Bee, A. Gupta, P. Tandon, Comparative vibrational spectroscopic studies, HOMO-LUMO and NBO analysis of N-(phenyl)-2, 2-dichloroacetamide, N-(2-chloro phenyl)-2, 2-dichloroacetamide and N-(4-chloro phenyl)-2,2-dichloroacetamide based on density functional theory, *Computational and Theoretical Chemistry*, 1016, 2016, 8-21.
- [24]. N. Sinha, O. Prasad, V. Naryan, S.R. Shukla, Raman, FT-IR spectroscopic analysis and first-order hyperpolarisability of 3-benzoyl-5-chlorouracil by first principles, *Journal of molecular simulations*, 37, 2011, 153-163.
- [25]. N.M. O'Boyle, A.L. Tenderholt, K.M. Langer, a library for package-independent computational chemistry algorithms, *Journal of computational chemistry*, 29, 2008, 839-845.
- [26]. P. Politzer, D.G. Truhlar (Eds.), Chemical Application of Atomic and Molecular Electrostatic Potentials, Plenum, New York, 1981
- [27]. P. Politzer and J. S. Murray, Molecular electrostatic potentials and chemical reactivity, *Reviews in computational chemistry*, 2, 1991, 273-279
- [28]. P. subhapiya, K. Sadasivam, M.L.N. Madhu mohan and P.S. Vijayanand, Experimental and theoretical investigation of p-n alkoxy benzoic acid based liquid crystal- A DFT approach, *Spectrochimica Acta Part A: Molecular and Biomolecular Spectroscopy*, 123, 2014, 511-523
- [29]. G. Mahalakshmi and V. Balachandran, NBO, HOMO, LUMO analysis and vibrational spectra (FTIR and FT-Raman) of 1-Amino 4-methylpiperazine using ab initio HF and DFT methods, *Spectrochimica Acta Part A: Molecular and Biomolecular Spectroscopy*, 135, 2015, 321-334.